



1 **Technical Note:**

2 **A two-sided affine power scaling relationship to represent the** 3 **concentration–discharge relationship**

4 José Manuel Tunqui Neira^{1,2}, Vazken Andréassian¹, Gaëlle Tallec¹ & Jean-Marie Mouchel²

5 ⁽¹⁾ Irstea, HYCAR Research Unit, Antony, France

6 ⁽²⁾ Sorbonne Université, CNRS, EPHE, UMR Metis 7619, Paris, France

7 **Abstract**

8 This technical note deals with the mathematical representation of concentration–discharge
9 relationships. We propose a two-sided affine power scaling relationship (2S-APS) as an alternative to
10 the classic one-sided power scaling relationship (commonly known as “power law”). We also discuss
11 the identification of the parameters of the proposed relationship, using an appropriate numerical
12 criterion. The application of 2S-APS to the high-frequency chemical time series of the Orgeval-Oracle
13 observatory is presented (in calibration and validation mode): It yields better results for several
14 solutes and for electrical conductivity in comparison with the power law relationship.

15 **Keywords**

16 Concentration–discharge relationships; log–log space; power law, high-frequency chemical data

17 **1. Introduction**

18 The relationship between solute concentrations and river discharge (from now on “C-Q relationship”)
19 is an age-old topic in hydrology (see among others Durum, 1953; Hem, 1948; Lenz and Sawyer, 1944).
20 It would be impossible to list here all the articles that have addressed this subject, and we refer our
21 readers to the most recent reviews (e.g., Bierozza et al., 2018; Botter et al., 2019; Moatar et al., 2017)
22 for an updated view of the ongoing research on C-Q relationships.

23 Many complex models have been proposed to represent C-Q relationships, from the tracer mass
24 balance (e.g., Minaudo et al., 2019) to the multiple regression methods (e.g., Hirsch et al., 2010).
25 Nonetheless, for the past 50 years the simple mathematical formalism known as “power law” has
26 enjoyed lasting popularity among hydrologists and hydrochemists (see, e.g., Edwards, 1973;
27 Gunnerson, 1967; Hall, 1970, 1971). Over the years, however, some shortcomings of this relationship
28 have become apparent: Recently, Minaudo et al. (2019) mentioned that, “fitting a single linear
29 regression on C-Q plots is sometimes questionable due to large dispersion in C-Q plots (even log



30 transformed)". Also, Moatar et al. (2017) present an extensive typology of shapes (in log–log space)
31 for the French national water quality database, which shows that the power law must be modified to
32 represent the C-Q relationship for dissolved components as well as for particulate-bound elements.

33 This technical note presents a two-sided affine power scaling relationship (named "2S-APS") that can
34 be seen as a generalization of the power law. And although we do not wish to claim that it can be
35 universally applicable, we argue here that it allows for a better description and modeling of the C-Q
36 relationship of some solutes as a natural extension of the power law.

37 **2. Test dataset**

38 We used the half-hourly (every 30 min) hydrochemical dataset collected by the in situ *River Lab*
39 laboratory at the Oracle-Orgeval observatory (Floury et al., 2017; Tallec et al., 2015). A short
40 description of the study site is given in Appendix 1. We used dissolved concentrations of three ions –
41 sodium [Na⁺], sulfate [S-SO₄²⁻], and chloride [Cl⁻] – as well as electrical conductivity (EC). This dataset
42 was collected from June 2015 to March 2018, averaging 20,700 measurement points.

43 As our main objective in this note is to compare the performance of two relationships (the new 2S-
44 APS and the classic power law), we divided our dataset into two parts to perform a split-sample test
45 (Klemeš, 1986): We used June 2015 to July 2017 for calibration (of both relationships), and August
46 2017 to March 2018 for validation. Table 1 presents the main characteristics of both periods.



47 **Table 1: Summary of high-frequency dissolved concentrations and electrical conductivity (EC;**
48 **average, minimum, maximum values and ratio between quantiles 90 and 10 divided by the mean)**
49 **from the River Lab at the Oracle-Orgeval observatory, divided into two groups: June 2015 to July**
50 **2017 (calibration period) and August 2017 to March 2018 (validation period).**

Solute	Unit	Calibration period (June 2015 to July 2017)			
		Mean (μ)	Min	Max	$(q_{90}-q_{10})/\mu$
Sodium	mg.L ⁻¹	13	2	17	0.22
Sulfate	Smg.L ⁻¹	19	2	32	0.44
Chloride	mg.L ⁻¹	30	4	40	0.28
EC	μ S.cm ⁻¹	704	267	1015	0.23

Validation period (August 2017 to March 2018)					
Solute	Unit	Mean (μ)	Min	Max	$(q_{90}-q_{10})/\mu$
Sodium	mg.L ⁻¹	13	3	17	0.59
Sulfate	Smg.L ⁻¹	18	3	26	0.70
Chloride	mg.L ⁻¹	29	4	40	0.71
EC	μ S.cm ⁻¹	576	171	813	0.65

51 **3. Mathematical formulations**

52 **3.1 Classic one-sided power scaling relationship (power law)**

53 Since at least 50 years ago, a one-sided power scaling relationship (commonly known as power law)
54 has been used to represent and model the relationship between solute concentration (C) and
55 discharge (Q) (Eq. (1)).

$$C = aQ^b \quad \text{Eq. (1)}$$

56 From a numerical point of view, the relationship presented in Eq. (1) is generally adjusted by first
57 transforming the dependent (C) and independent (Q) variables using a logarithmic transformation,
58 and then adjusting a linear model (Eq. (2)).

$$\ln(C) = \ln(a) + b \cdot \ln(Q) \quad \text{Eq. (2)}$$

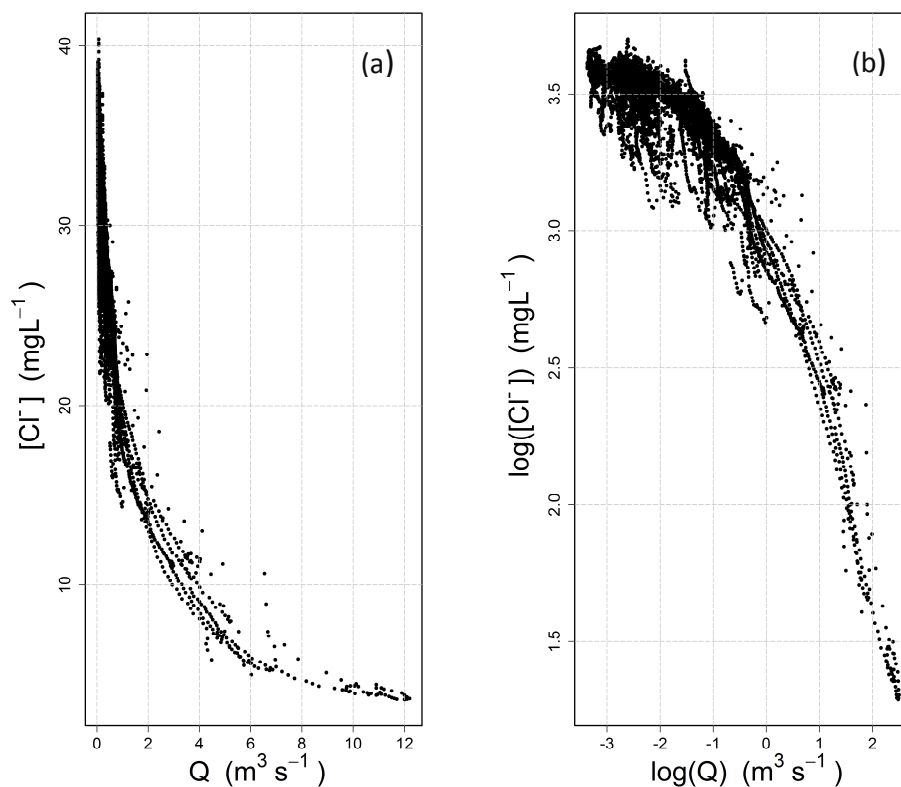
59 Graphically, this is equivalent to plotting concentration and discharge in a log–log space, where
60 parameters a and b can be identified either graphically or numerically, under the assumptions of
61 linear regression.

62 **3.2 Limits of the power law**

63 In many cases, the power law appears visually adequate (and conceptually simple), which explains its
64 lasting popularity. With the advent of high-frequency measuring devices in recent years, the size of



65 the datasets has exploded, and the C-Q relationship can now be analyzed on a wider span (Kirchner
66 et al., 2004). Figure 1 shows an example from our own high-frequency dataset: the 17,500 data
67 points (which correspond to the calibration period of Table 1) represent half-hourly measurements
68 collected over a 2-year period, during which the catchment was exposed to a variety of high- and
69 low-flow events, thus providing a great opportunity for exploring the shape of the C-Q relationship.
70 This being said, we do not wish to imply that a similar behavior could not been identified in medium-
71 and low-frequency datasets, which remain essential tools with which to analyze and understand
72 long-term hydrochemical processes (e.g., Godsey et al., 2009; Moatar et al., 2017).
73



74
75 **Figure 1: Concentration–discharge relationship observed at the Oracle-Orgeval observatory**
76 **(measurements from the River Lab) for chloride ions $[Cl^-]$: (a) standard axes, (b) logarithmic axes.**
77

78 Figure 1 illustrates the inadequateness of the power law for this dataset: The C-Q relationship
79 evolves from a well-defined concave shape on the left to a slightly convex shape on the right in the
80 log–log space. From the point of view of a modeler wishing to adjust a linear model, one has gone
81 beyond the straight shape that was aimed at. Note that this is true for our dataset, and that it does



82 not need to always be the case: The log–log space can be well adapted in some situations (see
83 examples in the paper by Moatar et al., 2017).

84 **3.3 A two-sided affine power scaling relationship as a progressive** 85 **alternative to the power law**

86 As a progressive alternative to the one-sided power scaling relationship (power law), we propose to
87 use a two-sided affine power scaling (2S-APS) relationship as shown in Eq. (3) (Box and Cox, 1964;
88 Howarth and Earle, 1979).

$$C^{\frac{1}{n}} = a + bQ^{\frac{1}{n}} \quad \text{Eq. (3)}$$

89 From a numerical point of view, the relationship presented in **Eq. (3)** is equivalent to first
90 transforming the dependent (C) and independent (Q) variables using a so-called Box–Cox
91 transformation (Box and Cox, 1964), and then adjusting a linear model. In comparison with the
92 logarithmic transformation, the additional degree of freedom offered by n allows for a range of
93 transformations, from the untransformed variable ($n = 1$) to the logarithmic transformation ($n \rightarrow \infty$).
94 This “progressive” property was underlined long ago by Box and Cox (1964): When n takes high
95 values, Eq. (3) converges toward the one-sided power scaling relationship (power law) (Eq. (1)). The
96 reason is simple:

$$C^{\frac{1}{n}} = e^{\frac{1}{n} \ln C} \approx 1 + \frac{1}{n} \ln C \quad \text{when } n \text{ is large.}$$

97 Thus, for large values of n , Eq. (3) can be written as:

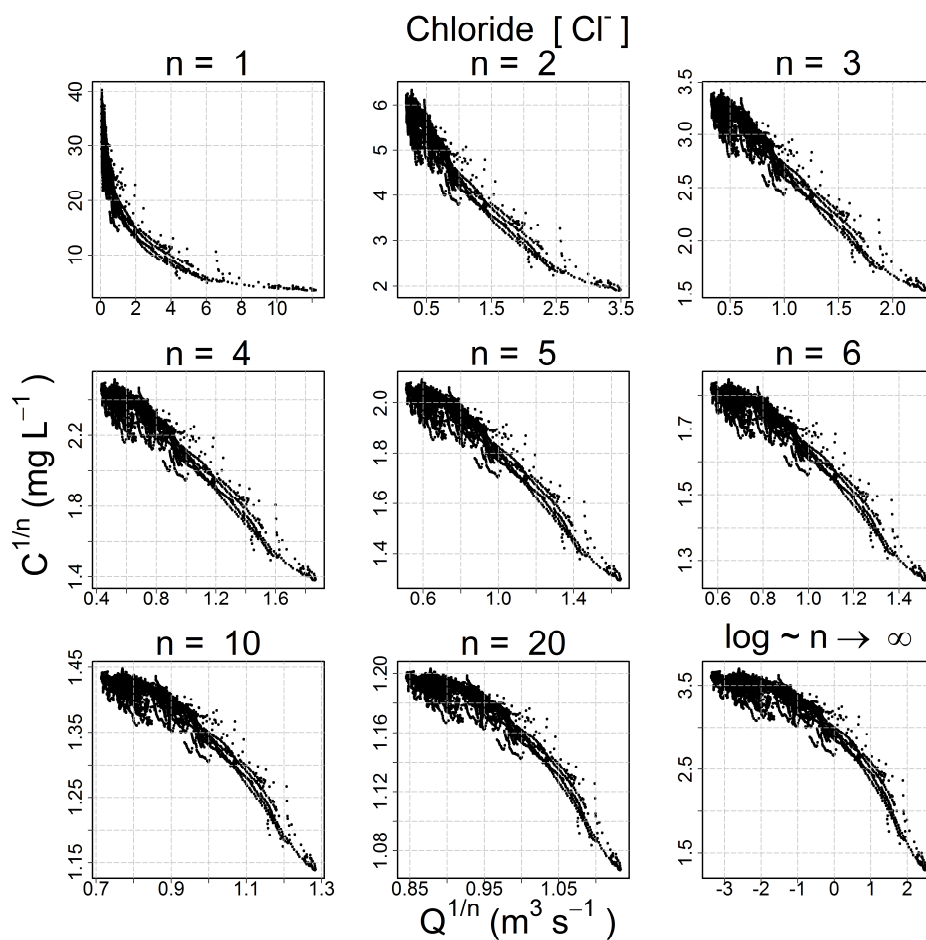
$$1 + \frac{1}{n} \ln C \approx a + b + \frac{b}{n} \ln Q$$

98 That is equivalent to:

$$\ln C \approx A + b \cdot \ln Q \quad (\text{with } A = n(a + b - 1))$$

99 The progressive behavior and the convergence toward the log–log space are clearly evident in Figure
100 2.

101



102

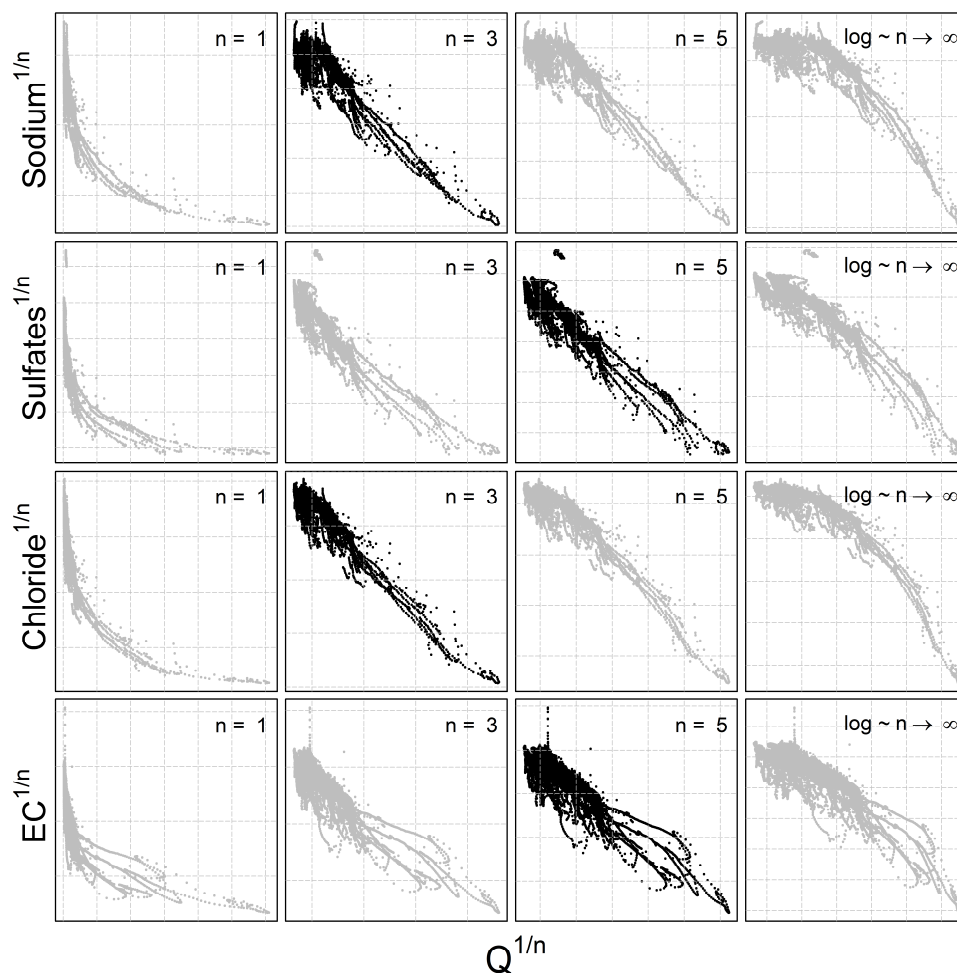
103 **Figure 2: Evolution of the shape of the concentration–discharge scatterplot for chloride ion with**
 104 **two-sided affine power scaling (2S-APS) and an increasing value of parameter n .**

105 **3.4 Choosing an appropriate transformation for different ion species**
 106 **(calibration mode)**

107 Because the hydro-biogeochemical processes that control the transport and reaction of ions are
 108 different, different ionic species may have a C-Q relationship of distinct shape (Moatar et al., 2017).
 109 In Figure 3, we show the behavior of three ions and the EC from the same catchment and the same
 110 dataset (all four from the Oracle-Orgeval observatory) with different transformations ($n=1, 3, 5$ and
 111 logarithmic transformation). The optimal shape was chosen numerically: We transformed our data
 112 series of C and Q using different values of n (i.e., $C^* = C^{1/n}$ and $Q^* = Q^{1/n}$) and logarithmic
 113 transformation (i.e., $C^{**} = \log(C)$ and $Q^{**} = \log(Q)$). With these transformed values, we performed



114 a linear regression and computed parameter a and b and the coefficient of determination (R^2) (see
115 Table 2). The n considered as optimal has the highest R^2 value (see Table 2). However, we could also
116 have followed the advice of Box et al. (2016, p. 331) and done it visually (Figure 3).
117



118
119 **Figure 3: C-Q behavior of three different chemical species and the electrical conductivity with**
120 **different 2S-APS transformations ($n=1, 3, 5$, and \log). The optimal power parameter (black dots)**
121 **was chosen based on the R^2 criterion. Note that we have removed the scale on the axes to focus**
122 **only on the change in shape in the C-Q relationship.**

123
124
125
126



127 **Table 2: Coefficient of determination (R^2) calculated for $n=1$ (no transformation), $n =$ optimal value**
128 **for two-sided affine power scaling relationship (Figure 3) and $n \rightarrow \infty$ (log–log space) for each ion**
129 **and for electrical conductivity (EC). Note that the R^2 is computed from transformed values.**

Solute	n	R^2
Sodium	$n = 1$ (no transformation)	0.53
	$n = 3$ (optimal)	0.73
	$n \rightarrow \infty$ (log–log)	0.53
Sulfate	$n = 1$ (no transformation)	0.32
	$n = 5$ (optimal)	0.81
	$n \rightarrow \infty$ (log–log)	0.77
Chloride	$n = 1$ (no transformation)	0.52
	$n = 3$ (optimal)	0.88
	$n \rightarrow \infty$ (log–log)	0.69
EC	$n = 1$ (no transformation)	0.38
	$n = 5$ (optimal)	0.79
	$n \rightarrow \infty$ (log–log)	0.74

130

131 The results given in Table 2 show the better quality of the fit obtained with the optimal value of n .

132 **4. Numerical identification of the parameters for the 2S-APS** 133 **relationship**

134 The extremely large number of values in this high-frequency dataset may cause problems for a
135 robust identification over the full range of discharges using a simple linear regression. Indeed, the
136 largest discharge values are in small numbers (in our dataset only 1% of discharges are in the range
137 [$2.6 \text{ m}^3\text{s}^{-1}$, $12.2 \text{ m}^3\text{s}^{-1}$], and they correspond to the lowest concentrations (see Figure 1)).

138 To address this question, we successively tested a large number of (a,b) pairs (n remaining fixed at
139 the optimal value given in Table 2). Each pair yields a series of simulated concentrations (C_{sim}) that
140 can be compared with the observed concentrations (C_{obs}). Among the many numerical criteria that
141 could be used, we chose the bounded version of the Nash and Sutcliffe (1970) efficiency criterion
142 $NSEB$ (Mathevet et al., 2006), which is commonly used in hydrological modeling. $NSEB$ can be
143 computed on concentrations or on discharge-weighted concentrations (which corresponds to the
144 load). We chose the average of both, because we found that it allows more weight to be given to the
145 extremely low concentrations and thus to avoid the issue of under-representation of high-
146 discharge/low-concentration measurement points. Table 3 presents the formula for these numerical
147 criteria.

148 We retained as optimal the pair of (a,b) that yielded the highest $NSEB_{comb}$ value (we explored in a
149 systematic fashion the range [1–5] for a and [–1.2–1.2] for b).



150 **Table 3: Numerical criteria used for optimization (C_{obs} – observed concentration, C_{sim} – simulated**
 151 **concentration, Q – observed discharge). The Nash and Sutcliffe (1970) efficiency (NSE) criterion is**
 152 **well known and widely used in the field of hydrology. The rescaling proposed by Mathevet et al.**
 153 **(2006) transforms NSE into NSEB, which varies between -1 and 1 (its optimal value). The advantage**
 154 **of this rescaled version is to avoid the occurrence of large negative values (the original NSE**
 155 **criterion varies in the range $[-\infty, 1]$).**

$$NSE_{conc} = 1 - \frac{\sum_t (C_{obs}^t - C_{sim}^t)^2}{\sum_t (C_{obs}^t - \bar{C}_{obs})^2} \quad \text{Eq. (4)}$$

$$NSEB_{conc} = \frac{NSE_{conc}}{2 - NSE_{conc}} \quad \text{Eq. (5)}$$

$$NSE_{load} = 1 - \frac{\sum_t (Q^t C_{obs}^t - Q^t C_{sim}^t)^2}{\sum_t (Q^t C_{obs}^t - \bar{Q} \bar{C}_{obs})^2} \quad \text{Eq. (6)}$$

$$NSEB_{load} = \frac{NSE_{load}}{2 - NSE_{load}} \quad \text{Eq. (7)}$$

$$NSEB_{comb} = \frac{1}{2} (NSEB_{conc} + NSEB_{load}) \quad \text{Eq. (8)}$$

156

157 5. Results

158 5.1 Results in calibration mode

159 The optimal values of a and b corresponding to the simulation of each ion and EC with the highest
 160 $NSEB_{comb}$ criterion and the n value identified in Figure 3 and Table 2 are presented in Table 4.

161 **Table 4: Summary of values a , b , and n used to obtain the optimal $NSEB_{comb}$ criterion.**

Ion	n	a	b	$NSEB_{comb}$
Sodium	3	2.70	-0.60	0.68
Sulfate	5	2.20	-0.55	0.69
Chloride	3	3.70	-1.00	0.83
EC	5	4.20	-0.70	0.77

162

163 For comparing the two relationships, we used the RMSE criterion. The results are shown in Table 5;
 164 they illustrate (for our catchment) the better performance (i.e., lower RMSE value) of the proposed
 165 2S-APS relationship for the three ions (sodium, sulfate, and chloride) over the power law
 166 relationship. For EC, there is a slight advantage over the power law. A test of the equality of variance
 167 (F-test) was performed between the RMSE obtained for the two relationships: Because of the very
 168 large number of points in our dataset, all differences were highly significant (p -value < 0.001)



169 **Table 5: Summary of values of RMSE criterion calculated for the three ions and EC.**

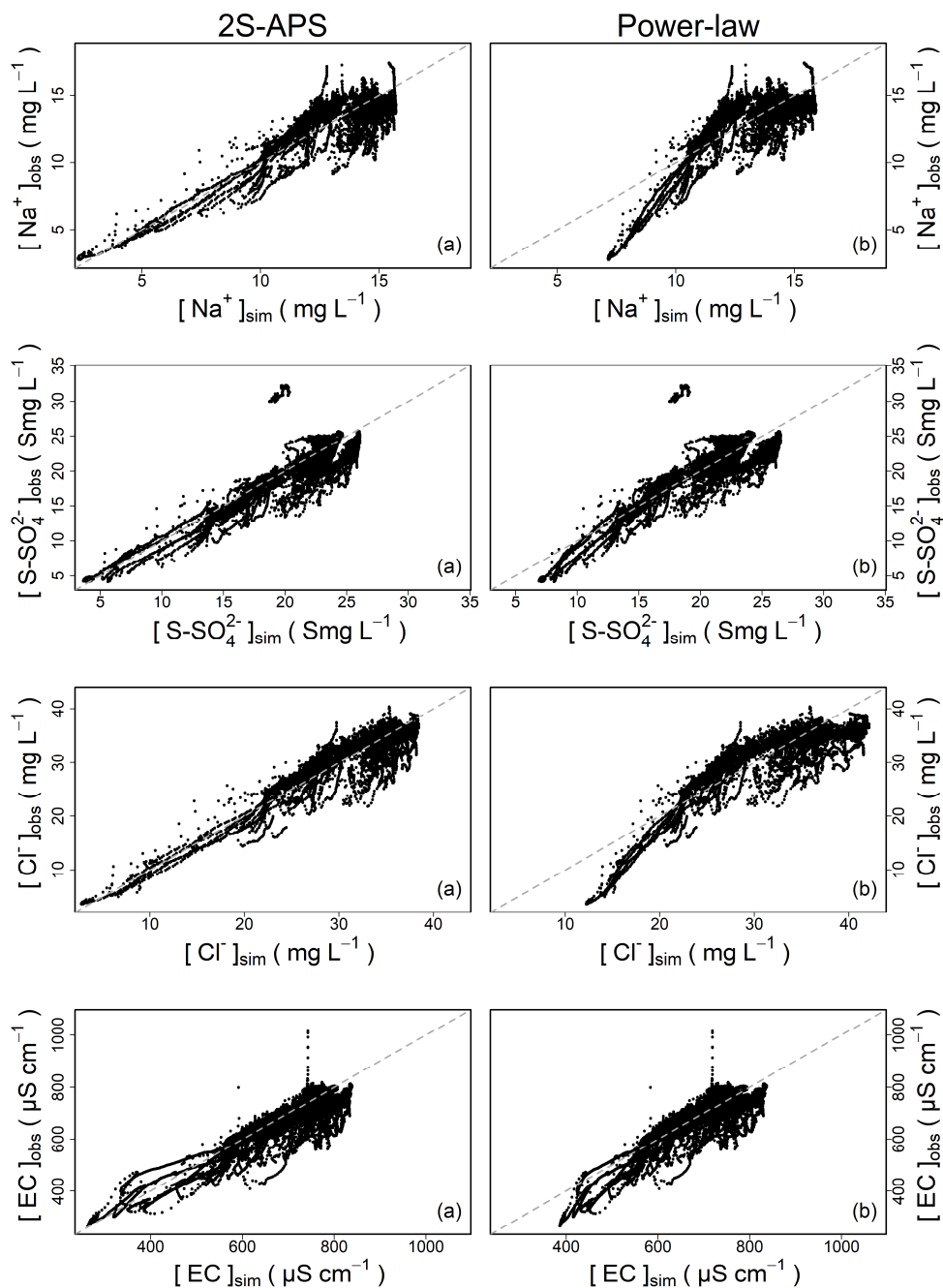
Solute	2S-APS	Power law
	RMSE	RMSE
Sodium	1.00 mgL ⁻¹	1.22 mgL ⁻¹
Sulfate	2.17 mgL ⁻¹	2.22 mgL ⁻¹
Chloride	2.00 mgL ⁻¹	2.91 mgL ⁻¹
EC	42.0 μS.cm ⁻¹	41.3 μS.cm ⁻¹

170

171 Figure 4 illustrates the comparison of the quality of simulation over the entire calibration dataset
172 between the power law and 2S-APS relationships. In general, the two-sided affine power scaling
173 relationship yields better simulated concentrations than the classic power law relationship for the
174 three ions (according to the results of Table 5). This is particularly evident over the low
175 concentrations. This better performance is more apparent in the case of sodium and chloride ions.



176



177

178 **Figure 4: Comparison of simulated concentrations with observed concentrations for: (a) two-sided**
 179 **affine power scaling (2S-APS) relationship, (b) power law (calibration mode).**



180 5.2 Results in validation mode

181 For the validation mode, we applied the above-calibrated relationships to a different time period
182 (August 2017 to March 2018). The results are shown in Table 6. The RMSE criterion illustrates (for
183 our catchment) the better performance of the proposed 2S-APS relationship over the power law
184 relationship for all the solutes. Unlike the calibration case, the quality of the simulation of EC using
185 the 2S-APS relationship has a much better performance than the one simulated by the power law
186 relationship.

187 **Table 6: Summary of values of RMSE criterion calculated for the three ions and EC with the**
188 **validation dataset.**

Solute	2S-APS	Power law
	RMSE	RMSE
Sodium	1.48 mgL ⁻¹	1.90 mgL ⁻¹
Sulfate	1.65 mgL ⁻¹	2.33 mgL ⁻¹
Chloride	3.69 mgL ⁻¹	4.34 mgL ⁻¹
EC	62.3 μS.cm ⁻¹	78.8 μS.cm ⁻¹

189

190 6. Conclusion

191 In this technical note, we tested and validated a three-parameter relationship (2S-APS) as an
192 alternative to the classic two-parameter one-sided power scaling relationship (commonly known as
193 “power law”), to represent the concentration–discharge relationship. We also proposed a way to
194 calibrate the 2S-APS relationship.

195 Our results (in calibration and validation mode) show that the 2S-APS relationship can be a valid
196 alternative to the power law: In our dataset, the concentrations simulated for sodium, sulfate, and
197 chloride as well as the EC are significantly better in validation mode, with a reduction in RMSE
198 ranging between 15 and 26%.

199

200 *Data availability.* Data will be available in a dedicated database website after a contract accepted on
201 behalf of all institutes.

202 *Competing interests.* The authors declare that they have no conflict of interest.

203 *Acknowledgments.* The first author acknowledges the Peruvian Scholarship Cienciactiva of CONCYTEC
204 for supporting his PhD study at Irstea and the Sorbonne University. The authors acknowledge the



205 EQUIPEX CRITEX program (grant no. ANR-11-EQPX-0011) for the data availability. We thank François
206 Bourgin for his kind review.

207

208 7. References

209 Bieroza, M. Z., Heathwaite, A. L., Bechmann, M., Kyllmar, K., and Jordan, P.: The concentration-
210 discharge slope as a tool for water quality management, *Science of The Total Environment*, 630, 738-
211 749, <https://doi.org/10.1016/j.scitotenv.2018.02.256>, 2018.

212 Botter, M., Burlando, P., and Fatichi, S.: Anthropogenic and catchment characteristic signatures in the
213 water quality of Swiss rivers: a quantitative assessment, *Hydrol. Earth Syst. Sci.*, 23, 1885-1904,
214 10.5194/hess-23-1885-2019, 2019.

215 Box, G. E., and Cox, D. R.: An analysis of transformations, *Journal of the Royal Statistical Society: Series B (Methodological)*, 26, 211-243, 1964.

217 Durum, W. H.: Relationship of the mineral constituents in solution to stream flow, Saline River near
218 Russell, Kansas, *Eos, Transactions American Geophysical Union*, 34, 435-442,
219 10.1029/TR034i003p00435, 1953.

220 Edwards, A. M. C.: The variation of dissolved constituents with discharge in some Norfolk rivers,
221 *Journal of Hydrology*, 18, 219-242, [https://doi.org/10.1016/0022-1694\(73\)90049-8](https://doi.org/10.1016/0022-1694(73)90049-8), 1973.

222 Floury, P., Gaillardet, J., Gayer, E., Bouchez, J., Tallec, G., Ansart, P., Koch, F., Gorge, C., Blanchouin,
223 A., and Roubaty, J. L.: The potamochemical symphony: new progress in the high-frequency
224 acquisition of stream chemical data, *Hydrol. Earth Syst. Sci.*, 21, 6153-6165, 2017.

225 Godsey, S. E., Kirchner, J. W., and Clow, D. W.: Concentration-discharge relationships reflect
226 chemostatic characteristics of US catchments, *Hydrological Processes*, 23, 1844-1864,
227 10.1002/hyp.7315, 2009.

228 Gunnerson, C. G.: Streamflow and quality in the Columbia River basin, *Journal of the Sanitary
229 Engineering Division*, 93, 1-16, 1967.

230 Hall, F. R.: Dissolved solids-discharge relationships .1. Mixing models, *Water Resources Research*, 6,
231 845-&, 10.1029/WR006i003p00845, 1970.

232 Hall, F. R.: Dissolved solids-discharge relationships .2. Applications to field data, *Water Resources
233 Research*, 7, 591-&, 10.1029/WR007i003p00591, 1971.

234 Hem, J. D.: Fluctuations in concentration of dissolved solids of some southwestern streams, *Eos,
235 Transactions American Geophysical Union*, 29, 80-84, 10.1029/TR029i001p00080, 1948.

236 Hirsch, R. M., Moyer, D. L., and Archfield, S. A.: Weighted Regressions on Time, Discharge, and
237 Season (WRTDS), with an Application to Chesapeake Bay River Inputs1, *JAWRA Journal of the
238 American Water Resources Association*, 46, 857-880, 10.1111/j.1752-1688.2010.00482.x, 2010.

239 Howarth, R., and Earle, S.: Application of a generalized power transformation to geochemical data,
240 *Journal of the International Association for Mathematical Geology*, 11, 45-62, 1979.



- 241 Kirchner, J. W., Feng, X., Neal, C., and Robson, A. J.: The fine structure of water-quality dynamics: the
242 (high-frequency) wave of the future, *Hydrological Processes*, 18, 1353-1359, 2004.
- 243 Klemeš, V.: Dilettantism in Hydrology: transition or destiny?, *Water Resour. Res.*, 22, 1775-1885,
244 1986.
- 245 Lenz, A., and Sawyer, C. N.: Estimation of stream-flow from alkalinity-determinations, *Eos*,
246 *Transactions American Geophysical Union*, 25, 1005-1011, 10.1029/TR025i006p01005, 1944.
- 247 Mathevet, T., Michel, C., Andreassian, V., and Perrin, C.: A bounded version of the Nash-Sutcliffe
248 criterion for better model assessment on large sets of basins, *IAHS PUBLICATION*, 307, 211, 2006.
- 249 Minaudo, C., Dupas, R., Gascuel-Oudou, C., Roubeix, V., Danis, P.-A., and Moatar, F.: Seasonal and
250 event-based concentration-discharge relationships to identify catchment controls on nutrient export
251 regimes, *Advances in Water Resources*, 131, 103379,
252 <https://doi.org/10.1016/j.advwatres.2019.103379>, 2019.
- 253 Moatar, F., Abbott, B., Minaudo, C., Curie, F., and Pinay, G.: Elemental properties, hydrology, and
254 biology interact to shape concentration-discharge curves for carbon, nutrients, sediment, and major
255 ions, *Water Resources Research*, 53, 1270-1287, 2017.
- 256 Nash, J. E., and Sutcliffe, J. V.: River flow forecasting through conceptual models part I—A discussion
257 of principles, *Journal of hydrology*, 10, 282-290, 1970.
- 258 Tallec, G., Ansard, P., Guérin, A., Delaigue, O., and Blanchouin, A.: Observatoire Oracle [Data set],
259 <https://dx.doi.org/10.17180/obs.oracle>, 2015.

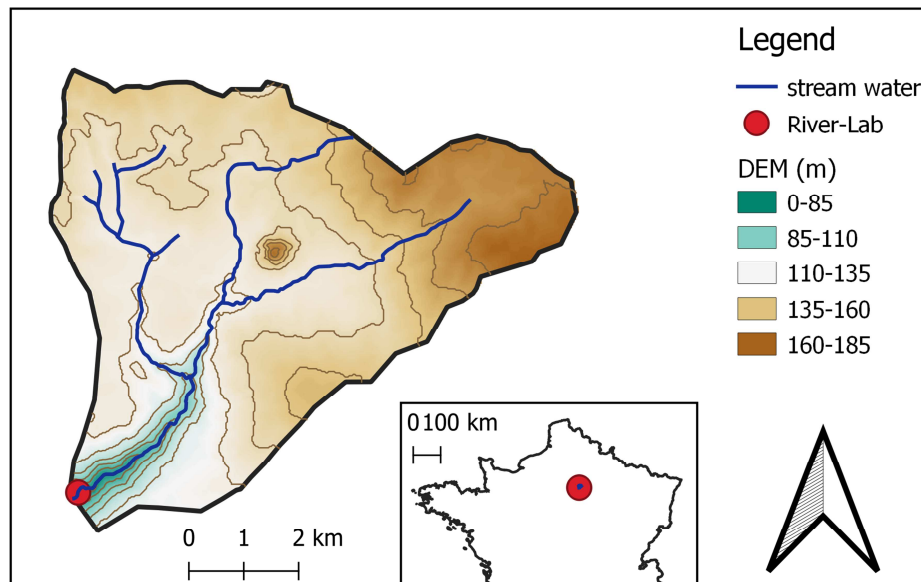
260

261

262 **8. Appendix 1 – Description of the River Lab**

263 In June 2015, the “River Lab” was deployed on the bank of the Avenelles River (within the limits of
264 the Oracle-Orgeval observatory, see Figure 5) to measure the concentration of all major dissolved
265 species at high frequency (Floury et al., 2017). The River Lab's concept is to “permanently” install a
266 series of laboratory instruments in the field in a confined bungalow next to the river. River Lab
267 performs a complete analysis every 30 min using two Dionex® ICS-2100 ionic chromatography (IC)
268 systems by continuous sampling and filtration of stream water. River Lab measures the concentration
269 of all major dissolved species ($[Mg^{2+}]$, $[K^+]$, $[Ca^{2+}]$, $[Na^+]$, $[Sr^{2+}]$, $[F^-]$, $[SO_4^{2-}]$, $[NO_3^-]$, $[Cl^-]$, $[PO_4^{3-}]$). In
270 addition, a set of physico-chemical probes is deployed to measure pH, conductivity, dissolved O_2 ,
271 dissolved organic carbon (DOC), turbidity, and temperature. The discharge is measured continuously
272 via a gauging station located at the River Lab site.

273 All the technical qualities, calibration of the equipment, comparison with laboratory measurements,
274 degree of accuracy, etc. have been well described in a publication by Floury et al. (2017).



275

276

Figure 5: Location of the River Lab (red dot) on the Avenelles River, Oracle-Orgeval observatory.

277